IEEE Access
Multidisciplinary | Rapid Review | Open Access Journal

Received July 21, 2021, accepted August 8, 2021, date of publication August 11, 2021, date of current version August 18, 2021.

Digital Object Identifier 10.1109/ACCESS.2021.3104020

Impact of Quality of Repairs and Common Cause Failures on the Reliability Performance of Intra-Bay IEC 61850 Substation Communication Network Architecture Based on Markov and Linear Dynamical Systems

VONANI CLIVE MATHEBULA AND AKSHAY KUMAR SAHA, (Member, IEEE)
Discipline of Electrical, Electronics and Computer Engineering, University of KwaZulu-Natal, Durban 4041, South Africa

Corresponding author: Akshay Kumar Saha (saha@ukzn.ac.za)

This work was supported by the School of Engineering, University of KwaZulu-Natal.

ABSTRACT Modernisation of substations using digital-based Substation Communication Networks (SCN) enables the automation of substations, allowing effective and efficient monitoring of substation equipment and implementing complex control and protection schemes. The IEC 61850 standard for SCN's objective is to integrate substation devices from different vendors, enabling peer-to-peer communication between the devices. The reliability investigation of the IEC 61850 based SCN architecture continues since it is left to the system designer to determine based on the network's applications and functions. In all endeavours to designing highly available SCN architectures, redundant systems are employed in mission-critical applications. In this paper, the impact of Common Cause Failures (CCF) and the quality of repairs on the reliability performance of IEC 61850 based architecture are investigated using the Markov process and Linear Dynamical Systems, where the diagnostic coverage level of the system is based on the ISO 13849-1. The results of the case studies indicate that common engineering design and coupling factors have a negative impact on the system reliability performance, notably for systems with high diagnostic coverage. The results also indicate that the factors have less impact when the system diagnostic coverage is low, specifically at low repair efficiency levels. However, the impact becomes more pronounced as the repair efficiency increases, as observed from the responses of the transition probability matrix's eigenvalue magnitudes. Thus, it is critical to ensure the minimum impact of common engineering design and coupling factors by diversifying the system's subsystems to ensure a high independence level.

INDEX TERMS Linear dynamical systems, Markov, IEC 61850, substation communication network (SCN), architecture, stability, reliability, common cause failures (CCFs), diagnostic coverage, repair efficiency.

NOMENCLATURE

β	Common Cause Failure.
Λ	Diagonal eigenvalue matrix.
γ	Eigenvalue.
V	Eigenvector matrix.
v	Eigenvector.
V	Eigenvector matrix.
λ	Failure rate.
Pr	Probability.
r_{eff}	Repair efficiency.
μ	Repair rate.
e_{dc}	System diagnostic coverage.
t	Time step.
P	Transition probability matrix.

ABBREVIATION

BB	Busbar.
CCF	Common Cause Failure.
CIT	Conventional Instrument Transformers.
HSR	Highly Available Seamless Redundancy.
IED	Intelligent Electronic Device.

The associate editor coordinating the review of this manuscript and approving it for publication was Yu Liu.

I/O	Input/output.
LDS	Linear Dynamical Systems.
NCIT	Non-Conventional Instrument Transformers.
MCS	Monte Carlo Simulation.
MU	Merging Unit.
MTTF	Mean Time To Failure.
MTTR	Mean Time To Repair.
OPNET	Optimised Network Engineering Tool.
PRP	Parallel Redundancy Protocol.
RBD	Reliability Block Diagram.
RSTP	Rapid Spanning Tree Protocol.
RTU	Remote Terminal Unit.
SCN	Substation Communication Network.
SW	Ethernet Switch.
SYNC	Synchroniser.
TS	Time synchronisation.

I. INTRODUCTION

Modernisation of substations using digital-based Substation Communication Networks (SCN) enables the automation of substations, allowing effective and efficient monitoring of substation equipment and implementing complex control and protection schemes [1], [2]. The IEC 61850 standard for SCN's objective is to integrate substation devices from different vendors, enabling peer-to-peer communication between the devices. Hence, mission-critical messages can be shared deterministically at the device level [3]. Moreover, the standard's architectural design allows distributed functions to be executed at bay-level, making the system reliable for executing protection functions. Even so, the reliability of the SCN architecture based on IEC 61850 continues to be investigated, considering that no specific architecture is mandatory. The architectural design of the IEC 61850 based SCN is left to the system designer to determine based on the criticality of the applications and functions of the network [1], [2]. In all endeavours to designing highly available SCN architectures, redundant systems are employed in mission-critical applications. The objective is to ensure that the individual scheme channels are independent, thereby ensuring hardware failures tolerance. However, many factors are making this goal to be unarchivable. The factors include system engineering, design, same location, same installation and commissioning teams, and same maintenance teams, resulting in Common Cause Factors (CCF). Thus, shared subsystems, components or algorithms in multi-channel systems introduce CCFs [4]–[8].

System engineering design, installation, commissioning, and maintenance are associated with root cause equipment failures, whereas the same engineering concept, same design, same installation team and same maintenance team make the equipment susceptible to the same root cause; which complicates reliability models [6], [8]–[11]. Nevertheless, integrating CCFs in SCN architecture reliability models is essential to accurately determine the reliability performance of the network [5], [12]. Belland [5] defines a single point of failure that causes a system to fail with a specified time simultaneously as a CCF, which is also used in the research work presented by the authors in [6], [9]. Common causes of failure and cascading failures are the contributing factors to system-dependent failures. Even so, both failure mechanisms are modelled as CCF in literature [8]–[10], [12], [13]. Therefore, both the dependent and cascading failures can be viewed as common stressors simultaneously affecting multiple subsystems or components in a system [4], [5], [9].

Modelling CCF as a proportion of a system's subsystems' failure rate simplifies reliability models [9], [14], subsequently improving the reliability performance accuracy of a system [6], [7], [13]. Various reliability models are used to model CCFs. Although the methods differ in their approach, they all quantify the level of dependent and independent system failures. In this paper, the beta model is used due to its simplicity to apply and comprehend [5], [9], [12], [14]. The contributions of the research are as follows:

a) Analysis of IEC 61850 SCN architecture reliability based on Markov process and Linear Dynamical Systems, considering the quality of repairs and common causes of failure; where the concept of architecture reliability focuses on the reliability of the physical SCN. In contrast, in general, the concept of reliability focuses on system reliability as a whole, including the protocol applied in the context of a SCN.
b) Impact of CCF on the system architectural state transitions' dynamics and stability, considering the quality of repairs.

Section II presents a critical review of IEC 61850 SCN architecture reliability studies. An overview of a synchronous generator protection system architecture and the study basis is presented in section III. Section IV presents the investigation methodology. The β-factor Markov reliability model used in this paper is discussed in Section V. Section VI presents Linear Dynamical System's concepts. The dynamical behaviour of the Markov process based on LDS is presented in section VII. Section VIII presents case study results and discussions. Finally, the findings and conclusions resulting from the research work are highlighted and discussed in Section IX.

II. A CRITICAL REVIEW OF IEC 61850 SCN ARCHITECTURE RELIABILITY STUDIES

Khavnekar *et al.* [15] presented a comparative study of IEC 61850 edition I and II, highlighting the reliability improvements in edition II considering a seamless network architecture reconfiguration based on the Parallel Redundancy Protocol (PRP) and Highly Available Seamless Redundancy (HSR) protocols. The authors in [16] discuss strategies and methods of improving SCN architecture reliability performance. Although the authors concur that PRP and HSR protocols offer high reliability, they also state the associated costs of implementing the architectures as the main disadvantage. According to A.T.A. Pereira *et al.* [16], PRP is expensive to implement than HSR even though it is considered

more reliable. Moreover, the two architectures are generally complex to implement and manage. However, the studies presented do not consider the impact of quality of repairs coupled with CCFs. The main advantage of PRP and HSR protocols is their deterministic performance due to their zero switchover time in case of a link failure [17], which is achieved by message frame detection and discarding of the duplicate frame at the destination device [18]. Ngo *et al.* [19] presents an algorithm that enhances the performance of the HSR protocol.

The application of IEC 61850 based SCN in a Substation Automation System (SAS) is demonstrated by Mnukwa and Saha [20]. The authors also demonstrated how external signals could be integrated into the SCN using RTU. Although the authors state that the SCN architecture used is reliable, the reliability evaluation of the SCN architecture is not discussed. *et al.* [21] and Zhang *et al.* [22] discuss the reliability performance of star, star-ring and redundant ring architectures based on the Reliability Block Diagram (RBD) method. The authors also presented a study of message communication efficiency using Optimised Network Engineering Tool (OPNET). They concluded that the star architecture is the most efficient to transmit messages but the least reliable considering hardware failure tolerance. The advantages and disadvantages presented by the authors do not consider the drawback of the RBD method failing to incorporate the quality of repairs [2], [23]. Another SCN architecture study focussing on the message transmission efficiency is presented by Das *et al.* [24]. The study, including the studies presented in [25]–[27], do not consider the impact of quality of repairs coupled with CCFs. The security aspects of IEC 61850 SCN based on IEC 62351-7 for network and system management are addressed by Albarakati *et al.* [28]. However, the authors do not relate the SCN security studies to the SCN architecture considering common causes of failure.

The reliability of SCN architectures integrating Conventional Instrument Transformers (CIT) and Non-Conventional Instrument Transformers (NCIT) is presented by Starck *et al.* [29], where the authors concluded that NCITs offer high-reliability performance than CITs on the SCN architecture using the RBD method [30], [31]. Kanabar and Sidhu [32] presents a similar study using the RBD method. The authors assume a zero network switchover on a link failure. However, RSTP protocol based on IEEE 802.1w is used, making it impossible to achieve a zero network switchover on a link failure. Mekkanen *et al.* [33] investigated the reliability performance of various IEC 61850 based SCN architectures using MCS. The MCS method enables various component failure distributions to be used simultaneously in the simulation, which improves the accuracy of the results. Nevertheless, the authors in [29], [32], [33] do not consider the impact of quality of repairs coupled with CCF on the reliability performance of the architecture.

Using the Markov process, Brand *et al.* [3] investigated IEC 61850 based SCN architectures for mission-critical applications. The study's outcome indicates that SCN architecture based on the IEC 61850 could be employed for executing safety-related functions. The drawback of the study is its lack of detail on the architecture used to implement the SCN, which could have possibly included the quality of repairs and CCFs. IEC 61850 based SCN architecture reliability is also investigated by Andersson *et al.* [34] using the Markov process. The authors concluded that IEC 61850 based SCN architectures are suitable to execute safety-related functions. In another study, Magro *et al.* [35] investigated the dependability of the IEC 61850 standard considering the requirements of the safety-related standard IEC 61508. Further studies in [36] concluded that all qualitative attributes of the IEC 61850 standards meet the requirements of the IEC 61508, as outlined in IEC 61784-3. In [23], the authors integrated the quality of repairs in a 'one-out-of-two' reliability model using the Markov process. The impact of the quality of repairs on the reliability performance of SCN architecture based on IEC 61850 is discussed in [37], [38]. Other studies presented by Mathebula and Saha [39], [40] focus on the SCN architecture's responsiveness to incremental changes in the quality of repairs. Nevertheless, the authors in [37]–[40] do not address the impact of CCF coupled with the quality of repairs on the SCN architecture. In this paper, the impact of quality of repairs coupled with CCFs on the SCN architectures is modelled using the Markov process and LDS. An overview of an power plant line feeder incorporating IEC 61850 SCN intra-bay architecture is presented in the following section and is the study basis presented herein. The following section presents an overview of the IEC 61850 based SCN intra-bay architecture of a synchronous generator serving as a basis for the study presented herein.

III. OVERVIEW OF SYNCHRONOUS GENERATOR PROTECTION SYSTEM ARCHITECTURE AND STUDY BASIS

Figure 1 depicts a 'one-out-of-two' generator protection scheme SCN's architecture with a synchronising functionality comprising two selectable synchronisers. The scheme comprises two identical SCN architectures interfacing to the primary plant CITs' through Merging Units (MU) at the process bus level [44]. The protection scheme SCN architecture depicted in Figure 1 covers the essential protection functions and provides the closing supervision of the generator circuit breaker when synchronising to the grid. In addition, enabling any of the synchronisers to be selectable adds complexity in modelling the system dynamics, allowing the capability of the proposed modelling approach to be fully demonstrated. The complexity level is also balanced by what can be implemented in practice, assuming that the circuit breaker has a main and backup trip coils to successfully integrate into a ''one-out-of-two'' scheme.

The MTTF data of the scheme's SCN devices is presented in Table 1, where 8 hours is assumed to be the MTTR of the SCN devices [32].

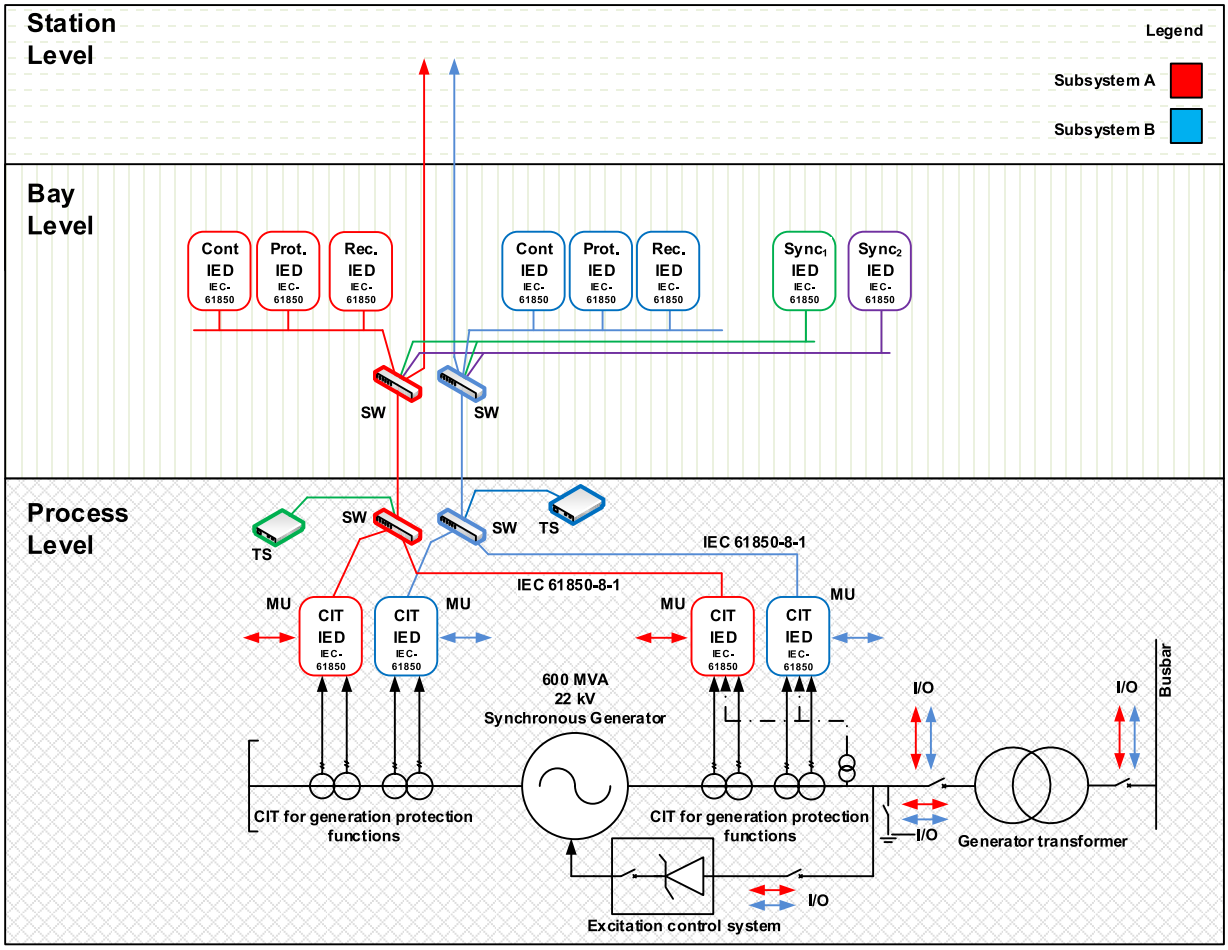

FIGURE 1. Synchronous generator based on IEC-61850 SCN [41]–[43].

TABLE 1. Mean time to failure data of substation devices [32].

Intra-bay Substation Communication Network Devices	MTTF (Years)
Protection IED	150
Control IED	150
Disturbance Recorder IED	150
Ethernet switch (SW)	50
Synchroniser (SYNC)	150
Time synchronisation (TS)	150
Merging Unit (MU)	150

IV. METHODOLOGY

The modelling approach followed in this paper considers a group of components where a failure of one component results in a loss of the intended functionality of the subsystem. Subsystems A and B are independent, identical subsystems of a one-out-of-two generator protection scheme, where either synchroniser supervises the closing of the generator circuit breaker. Synchronisers 1 or 2 are referred to as subsystems C and D depicted in Figure 1. The Merging Units (MU), Time synchroniser (TS), switches, protection, recorder, and control IEDs are subcomponents of the individual subsystems A and B. These systems are required for the functionality of the individual subsystems, as depicted in Figure 2, assuming that the two systems A and B are entirely independent of each other, where each MU and TS, SW and IED have their MTTF and MTTR values. The RBD method is used to calculate the MTTF of the individual subsystems. Thus, The subsystem can be modelled as having an MTTF and MTTR. In the system under consideration, CCFs are modelled by a block in series with two paralleled subsystems A and B. Thereafter, to incorporate the quality of repairs (viz. repair efficiency and diagnostic coverage), the RBD of the system is then transformed into a Markov process, which enables the determination of the system's transient states.

The asymptotic behaviour of the system is investigated using the concept of LDS, where the system's state space represents the Markov partitions of the system [45]. This approach enables the system dynamics to be investigated based on the eigenvalues of the transition probability matrix [46]. Figure 3 depicts the research methodology flowchart followed in this paper.

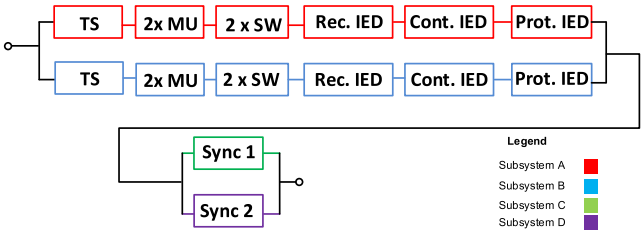

FIGURE 2. Reliability block diagram of 'one-out-of-two' scheme [32].

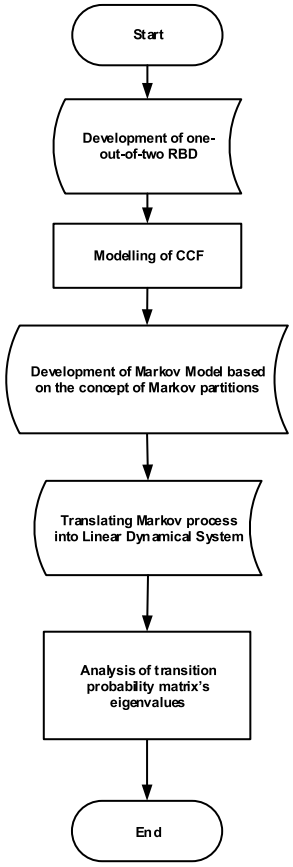

FIGURE 3. Investigation methodology flowchart.

V. MARKOV PROCESS RELIABILITY MODEL

The Markov process reliability model of the RBD of Figure 2 is depicted in Figure 4 using the subsystem's transfer rates concept between any two connected system states [47], where e_{dc}, r_{eff}, μ and λ are the diagnostic coverage, repair efficiency, repair rate and failure rate [23], [37]. To account for imperfect repairs due to the diagnostic capability factor and repair efficiency within the subsystems, two factors (viz. diagnostic coverage (e_{dc}) and repair efficiency (r_{eff})) are respectively introduced for the individual subsystems, as depicted in Figure 4. Thus, whenever subsystem A, B, C or D fails (i.e., states S-2, S-3, S-4 or S-5), the respective subsystem repair rate (μ) is multiplied by the diagnostic capability factor and the repair efficiency to account for the identified system faults and the correctness and completeness. An additional component modifies the subsequent subsystem failure rates from states S-2, S-3, S-4 or S-5 ($\mu_A(1-e_{dcA})$, $\mu_B(1-e_{dcB})$, $\mu_C(1-e_{dcC})$ and $\mu_D(1-e_{dcD})$), respectively, due to the unidentified faults within the subsystems. Thus, the components represent the unaccounted portions of subsystem A and subsystem B repairs, which increases the failure probability over time.

The functional states of the system are represented by state S-1, which is a fully functional state of the protection scheme. States S-2 to S-9 represent partial systems availability, whereas state S-10 represents a complete scheme failure. Therefore, the sum of states S-1 to S-9 probabilities represents the system's availability [37]. The beta factor model is used in this paper due to its simplicity to comprehend and apply to incorporate the CCF impact in the reliability model of Figure 4 [4], [5], [9]. Moreover, the scheme's channels under consideration are considered identical (viz. A and B, as well as C and D), thereby making the beta factor model suitable. The beta factor model attributes a fraction of the subsystem's failure rate to the CCF component as a single parameter model [48]. In order to demonstrate the application of the beta factor model, a 'one-out-of-two' scheme with common causes of failure is considered, as depicted in Figure 5, where $f(\lambda_A, \lambda_B)$ is an averaging function of the subsystem's failure rates, representing failures that could be related to design considerations (root causes) or coupling factors, considering the dependence level of the system.

Consequently, the Markov process of the system representing CCFs transfer rates is depicted in Figure 6, where the matrix gives the system's state transition rate matrix (1).

$$P_\beta = \begin{bmatrix} 1-(1-\beta)\lambda_A-(1-\beta)\lambda_B-\beta f(\lambda_A,\lambda_B) & (1-\beta)\lambda_A & (1-\beta)\lambda_B & \beta f(\lambda_A,\lambda_B) \\ 0 & 1-\lambda_B & 0 & \lambda_B \\ 0 & 0 & 1-\lambda_A & \lambda_A \\ 0 & 0 & 0 & 1 \end{bmatrix} \quad (1)$$

Although the CCF rate ($\beta f(\lambda_A, \lambda_B)$,) of the subsystems is modelled as a percentage of the subsystem's failure rate, it can also be modelled as a sum of dependent and independent failure causes, where the increase of the CCF increases the transfer rate of the subsystem. Thus, leading to the same results since a decrease in $(1-\beta)\lambda_A$ increases $\beta f(\lambda_A, \lambda_B)$, leading to lower reliability because the system can easily transition into the failure state S-4. Similarly, the state transition rate matrix of the system depicted in Figure 4 incorporating CCFs are given by (2), as shown at the bottom of the page 7 and depicted in Figure 7, of which the state functional and non-functional states are presented in Table 2.

where the entries P_{ii} for $i = i$ are given by (3) to (11) below to ease the readability of the equation.

$$P_{11} = 1-(1-\beta)\lambda_A-(1-\beta)\lambda_B-(1-\beta)\lambda_C - (1-\beta)\lambda_D-\beta f(\lambda_A,\lambda_B,\lambda_C,\lambda_D) \quad (3)$$

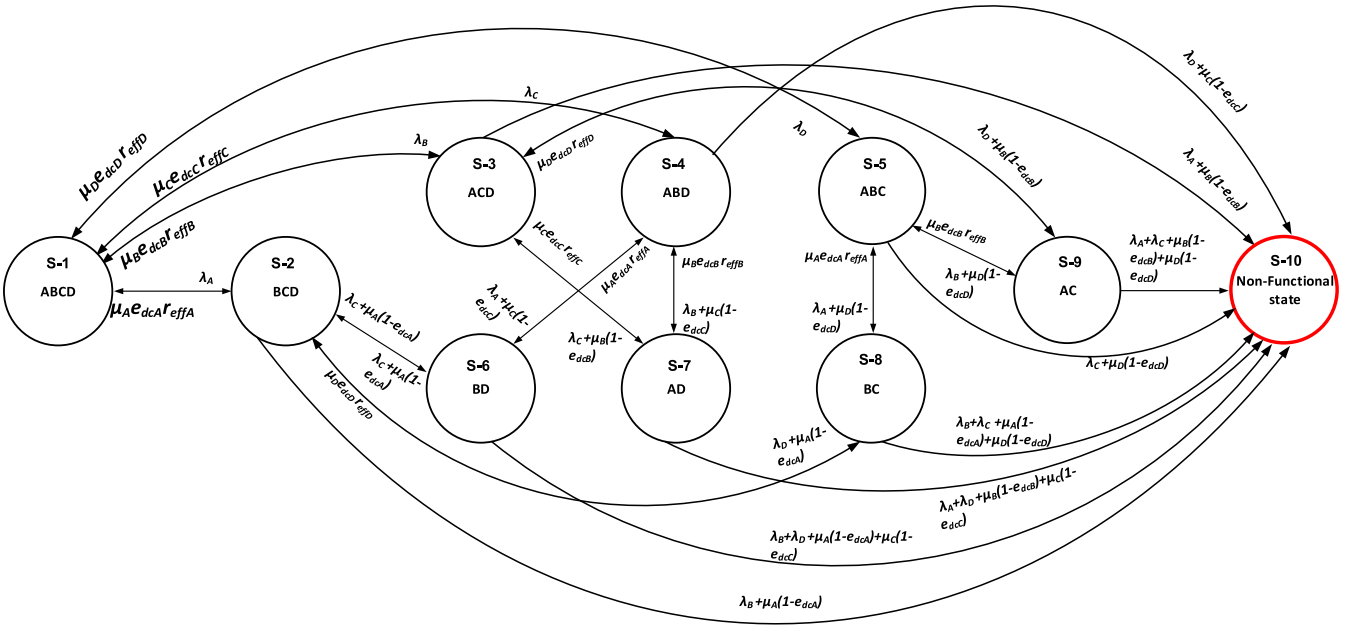

FIGURE 4. Markov process reliability model of a synchronous generator protection scheme.

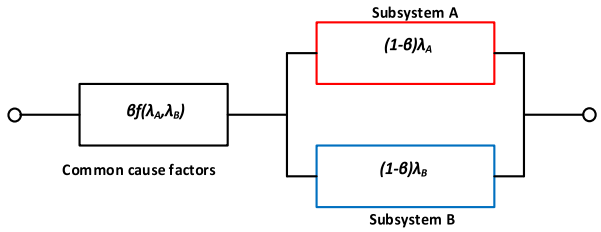

FIGURE 5. Reliability block diagram model of 'one-out-of-two' system incorporating CCFs based on the β-factor model.

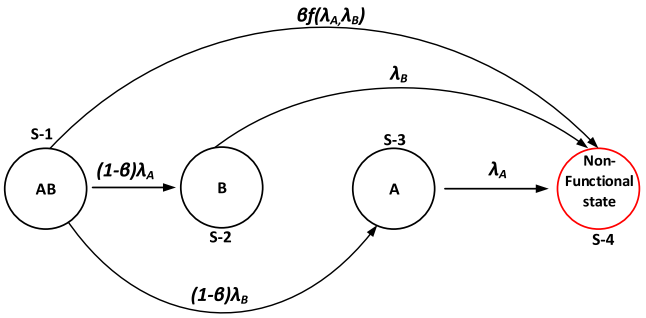

FIGURE 6. Markov model of 'one-out-of-two' system failure probabilities incorporating CCFs based on the β factor model.

TABLE 2. Functional and non-functional system states.

Subsystems				System state	State No.
A	B	C	D		
0	0	0	0	Non-Functional	**10**
0	0	0	1	Non-Functional	**10**
0	0	1	0	Non-Functional	**10**
0	0	1	1	Non-Functional	**10**
0	1	0	0	Non-Functional	**10**
0	1	0	1	Functional	**6**
0	1	1	0	Functional	**8**
0	1	1	1	Functional	**2**
1	0	0	0	Non-Functional	**10**
1	0	0	1	Functional	**7**
1	0	1	0	Functional	**9**
1	0	1	1	Functional	**3**
1	1	0	0	Non-Functional	**10**
1	1	0	1	Functional	**4**
1	1	1	0	Functional	**5**
1	1	1	1	Functional	**1**

$$P_{22} = 1 - ((1-\beta)\lambda_C + \mu_A(1-e_{dcA})) - ((1-\beta)\lambda_D + \mu_A(1-e_{dcA})) - (\lambda_B + \mu_A(1-e_{dcA}) + \beta f(\lambda_C, \lambda_D)) \quad (4)$$

$$P_{33} = 1 - ((1-\beta)\lambda_C + \mu_B(1-e_{dcB})) - ((1-\beta)\lambda_D + \mu_B(1-e_{dcB})) - (\lambda_A + \mu_B(1-e_{dcB}) + \beta f(\lambda_C, \lambda_D)) \quad (5)$$

$$P_{44} = 1 - ((1-\beta)\lambda_A + \mu_C(1-e_{dcC})) - ((1-\beta)\lambda_B + \mu_C(1-e_{dcC})) - (\lambda_D + \mu_C(1-e_{dcC}) + \beta f(\lambda_A, \lambda_B)) \quad (6)$$

$$P_{55} = 1 - \left((1-\beta)\lambda_A + \mu_D(1-e_{dcD})\right) - ((1-\beta)\lambda_B + \mu_D(1-e_{dcD})) - (\lambda_C + \mu_D(1-e_{dcD}) + \beta f(\lambda_A, \lambda_B)) \quad (7)$$

$$P_{66} = 1 - (\lambda_B + \lambda_D + \mu_A(1-e_{dcA}) + \mu_C(1-e_{dcC})) \quad (8)$$

$$P_{77} = 1 - (\lambda_A + \lambda_D + \mu_B (1 - e_{dcB}) + \mu_C (1 - e_{dcC})) \quad (9)$$

$$P_{88} = 1 - (\lambda_B + \lambda_C + \mu_A (1 - e_{dcA}) + \mu_D (1 - e_{dcD})) \quad (10)$$

$$P_{99} = 1 - (\lambda_A + \lambda_C + \mu_B (1 - e_{dcB}) + \mu_D (1 - e_{dcD})) \quad (11)$$

In the model presented in this paper, all non-functional states are grouped into one system state, where a system "failure" is represented by state S-10 in the model. This approach enables the reduction of the total states in the system from sixteen to only ten, which would be of interest to maintenance and operating personnel. Therefore, incorporating the impact of CCFs, as depicted in Figure 7 into Figure 4, leads to a modified Markov state probability diagram, as depicted in Figure 8. The matrix in (12), as shown at the bottom of the next page describes the state transition rates of the process, where the system is assumed to be fully functional at the beginning of the simulation. The following section presents the main concepts of LDS used to study repairs quality impact with CCFs on the reliability performance of the protection scheme's SCN architecture.

where the entries P_{ii} for $i = i$ are given by (13) to (21) below to ease the readability of the equation.

$$P_{11} = 1 - (1 - \beta)\lambda_A - (1 - \beta)\lambda_B - (1 - \beta)\lambda_C - (1 - \beta)\lambda_D - \beta f(\lambda_A, \lambda_B, \lambda_C, \lambda_D) \quad (13)$$

$$P_{22} = 1 - ((1 - \beta)\lambda_C + \mu_A (1 - e_{dcA})) - ((1 - \beta)\lambda_D + \mu_A (1 - e_{dcA})) - (\lambda_B + \mu_A (1 - e_{dcA}) + \beta f(\lambda_C, \lambda_D)) - \mu_A e_{dcA} r_{effA} \quad (14)$$

$$P_{33} = 1 - \big((1 - \beta)\lambda_C + \mu_B(1 - e_{dcB})\big) - \big((1 - \beta)\lambda_D + \mu_B(1 - e_{dcB})\big) - \big(\lambda_A + \mu_B(1 - e_{dcB})\&\ + \beta f(\lambda_C, \lambda_D)\big) - \mu_B e_{dcB} r_{effB} \quad (15)$$

$$P_{44} = 1 - \big((1 - \beta)\lambda_A + \mu_C(1 - e_{dcC})\big) - \big((1 - \beta)\lambda_B + \mu_C(1 - e_{dcC})\big) - \big(\lambda_D + \mu_C(1 - e_{dcC}) + \beta f(\lambda_A, \lambda_B)\big) - \mu_C e_{dcC} r_{effC} \quad (16)$$

$$P_{55} = 1 - \big((1 - \beta)\lambda_A + \mu_D(1 - e_{dcD})\big) - \big((1 - \beta)\lambda_B + \mu_D(1 - e_{dcD})\big) - \big(\lambda_C + \mu_D(1 - e_{dcD}) + \beta f(\lambda_A, \lambda_B)\big) - \mu_D e_{dcD} r_{effD} \quad (17)$$

$$P_{66} = 1 - \big(\lambda_B + \lambda_D + \mu_A(1 - e_{dcA}) + \mu_C(1 - e_{dcC})\big) - \mu_C e_{dcC} r_{effC} - \mu_A e_{dcA} r_{effA} \quad (18)$$

$$P_{77} = 1 - \big(\lambda_A + \lambda_D + \mu_B(1 - e_{dcB}) + \mu_C(1 - e_{dcC})\big) - \mu_C e_{dcC} r_{effC} - \mu_B e_{dcB} r_{effB} \quad (19)$$

$$P_{88} = 1 - \big(\lambda_B + \lambda_C + \mu_A(1 - e_{dcA}) + \mu_D(1 - e_{dcD})\big) - \mu_D e_{dcD} r_{effD} - \mu_A e_{dcA} r_{effA} \quad (20)$$

$$P_{99} = 1 - \big(\lambda_A + \lambda_C + \mu_B(1 - e_{dcB}) + \mu_D(1 - e_{dcD})\big) - \mu_D e_{dcD} r_{effD} - \mu_B e_{dcB} r_{effB} \quad (21)$$

VI. LINEAR DYNAMICAL SYSTEMS

This section presents the main concepts used in this paper to study the system's dynamics, considering the state transition movements as a series of finite symbols. At the highest level of system abstraction, it is considered that the next system's state is only dependent on the current state based on some rule, such that the next system state is given by (22), assuming that x is a vector in R^n, where n represents the dimension of the system if a linear map exists such that $X : R^n \rightarrow R^n$ [38], [49]–[51].

$$x_{n+1} = X(x_n) \quad (22)$$

$$P_\beta = \begin{bmatrix} P_{11} & (1-\beta)\lambda_A & (1-\beta)\lambda_B & (1-\beta)\lambda_C & (1-\beta)\lambda_D & 0 & 0 & \cdots \\ 0 & P_{22} & 0 & 0 & 0 & (1-\beta)\lambda_C + \mu_A(1-e_{dcA}) & 0 & \\ 0 & 0 & P_{33} & 0 & 0 & 0 & (1-\beta)\lambda_C + \mu_B(1-e_{dcB}) & \\ 0 & 0 & 0 & P_{44} & 0 & (1-\beta)\lambda_A + \mu_C(1-e_{dcC}) & (1-\beta)\lambda_B + \mu_C(1-e_{dcC}) & \\ 0 & 0 & 0 & 0 & P_{55} & 0 & 0 & \\ 0 & 0 & 0 & 0 & 0 & P_{66} & 0 & \\ 0 & 0 & 0 & 0 & 0 & 0 & P_{77} & \\ 0 & 0 & 0 & 0 & 0 & 0 & 0 & \\ 0 & 0 & 0 & 0 & 0 & 0 & 0 & \\ 0 & 0 & 0 & 0 & 0 & 0 & 0 & \end{bmatrix}$$

$$\begin{bmatrix} 0 & 0 & \beta f(\lambda_A, \lambda_B, \lambda_C, \lambda_D) \\ (1-\beta)\lambda_D + \mu_A(1-e_{dcA}) & 0 & \lambda_B + \mu_A(1-e_{dcA}) + \beta f(\lambda_C, \lambda_D) \\ 0 & (1-\beta)\lambda_D + \mu_B(1-e_{dcB}) & \lambda_A + \mu_B(1-e_{dcB}) + \beta f(\lambda_C, \lambda_D) \\ 0 & 0 & \lambda_D + \mu_C(1-e_{dcC}) + \beta f(\lambda_A, \lambda_B) \\ (1-\beta)\lambda_A + \mu_D(1-e_{dcD}) & (1-\beta)\lambda_B + \mu_D(1-e_{dcD}) & \lambda_C + \mu_D(1-e_{dcD}) + \beta f(\lambda_A, \lambda_B) \\ 0 & 0 & \lambda_B + \lambda_D + \mu_A(1-e_{dcA}) + \mu_C(1-e_{dcC}) \\ 0 & 0 & \lambda_A + \lambda_D + \mu_B(1-e_{dcB}) + \mu_C(1-e_{dcC}) \\ P_{88} & 0 & \lambda_B + \lambda_C + \mu_A(1-e_{dcA}) + \mu_D(1-e_{dcD}) \\ 0 & P_{99} & \lambda_A + \lambda_C + \mu_B(1-e_{dcB}) + \mu_D(1-e_{dcD}) \\ 0 & 0 & 1 \end{bmatrix} \quad (2)$$

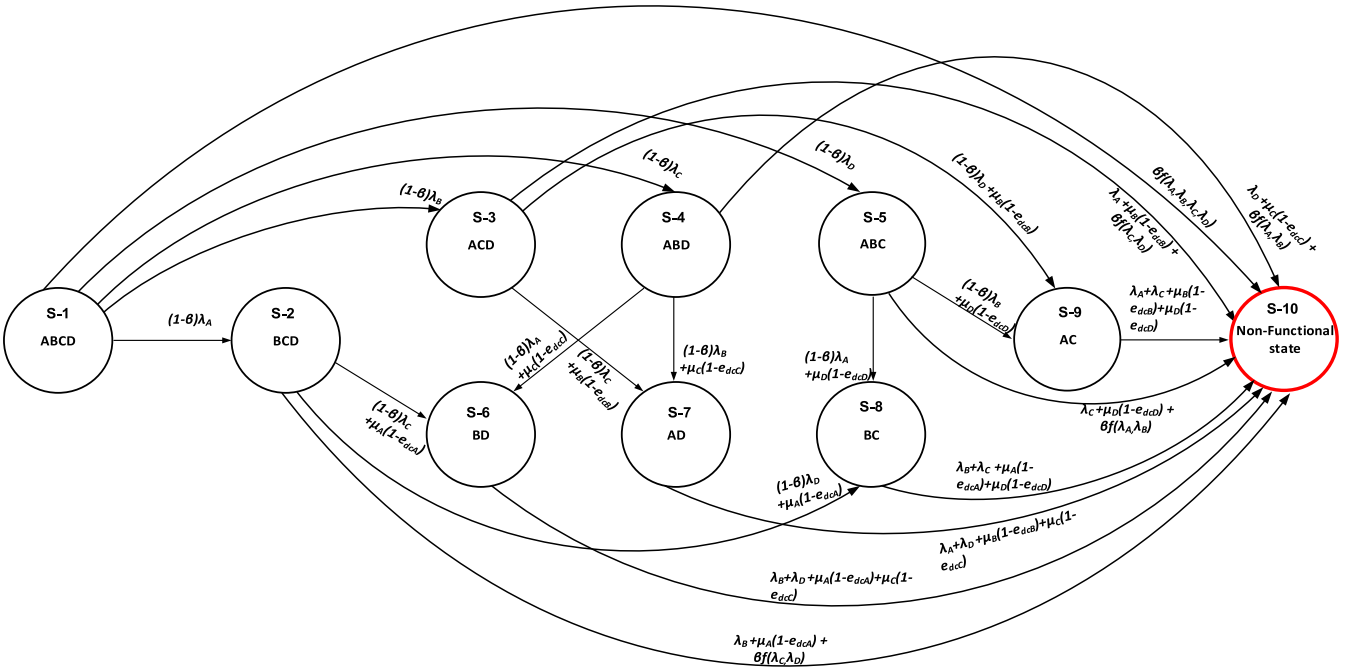

FIGURE 7. Markov model of synchronous generator failure probabilities incorporating CCFs based on the β factor model.

$$
P = \begin{bmatrix}
P_{11} & (1-\beta)\lambda_A & (1-\beta)\lambda_B & (1-\beta)\lambda_C & (1-\beta)\lambda_D & 0 & \cdots \\
\mu_A e_{dcA} r_{effA} & P_{22} & 0 & 0 & 0 & (1-\beta)\lambda_C + \mu_A(1-e_{dcA}) & \\
\mu_B e_{dcB} r_{effB} & 0 & P_{33} & 0 & 0 & 0 & \\
\mu_C e_{dcC} r_{effC} & 0 & 0 & P_{44} & 0 & (1-\beta)\lambda_A + \mu_C(1-e_{dcC}) & \\
\mu_D e_{dcD} r_{effD} & 0 & 0 & 0 & P_{55} & 0 & \\
0 & \mu_C e_{dcC} r_{effC} & 0 & \mu_A e_{dcA} r_{effA} & 0 & P_{66} & \\
0 & 0 & \mu_C e_{dcC} r_{effC} & \mu_B e_{dcB} r_{effB} & 0 & 0 & \\
0 & \mu_D e_{dcD} r_{effD} & 0 & 0 & \mu_A e_{dcA} r_{effA} & 0 & \\
0 & 0 & \mu_D e_{dcD} r_{effD} & 0 & \mu_B e_{dcB} r_{effB} & 0 & \\
0 & 0 & 0 & 0 & 0 & 0 &
\end{bmatrix}
$$

$$
\begin{bmatrix}
0 & 0 & 0 & \\
0 & (1-\beta)\lambda_D + \mu_A(1-e_{dcA}) & 0 & \\
(1-\beta)\lambda_C + \mu_B(1-e_{dcB}) & 0 & (1-\beta)\lambda_D + \mu_B(1-e_{dcB}) & \\
(1-\beta)\lambda_B + \mu_C(1-e_{dcC}) & 0 & 0 & \\
0 & (1-\beta)\lambda_A + \mu_D(1-e_{dcD}) & (1-\beta)\lambda_B + \mu_D(1-e_{dcD}) & \\
0 & 0 & 0 & \\
P_{77} & 0 & 0 & \\
0 & P_{88} & 0 & \\
0 & 0 & P_{99} & \\
0 & 0 & 0 &
\end{bmatrix}
\begin{bmatrix}
\cdots \\ \\ \\ \\ \cdots \\ \\ \\ \\ \\ \\
\end{bmatrix}
\begin{bmatrix}
\beta f(\lambda_A, \lambda_B, \lambda_C, \lambda_D) \\
\lambda_B + \mu_A(1-e_{dcA}) + \beta f(\lambda_C, \lambda_D) \\
\lambda_A + \mu_B(1-e_{dcB}) + \beta f(\lambda_C, \lambda_D) \\
\lambda_D + \mu_C(1-e_{dcC}) + \beta f(\lambda_A, \lambda_B) \\
\lambda_C + \mu_D(1-e_{dcD}) + \beta f(\lambda_A, \lambda_B) \\
\lambda_B + \lambda_D + \mu_A(1-e_{dcA}) + \mu_C(1-e_{dcC}) \\
\lambda_A + \lambda_D + \mu_B(1-e_{dcB}) + \mu_C(1-e_{dcC}) \\
\lambda_B + \lambda_C + \mu_A(1-e_{dcA}) + \mu_D(1-e_{dcD}) \\
\lambda_A + \lambda_C + \mu_B(1-e_{dcB}) + \mu_D(1-e_{dcD}) \\
1
\end{bmatrix}
\tag{12}
$$

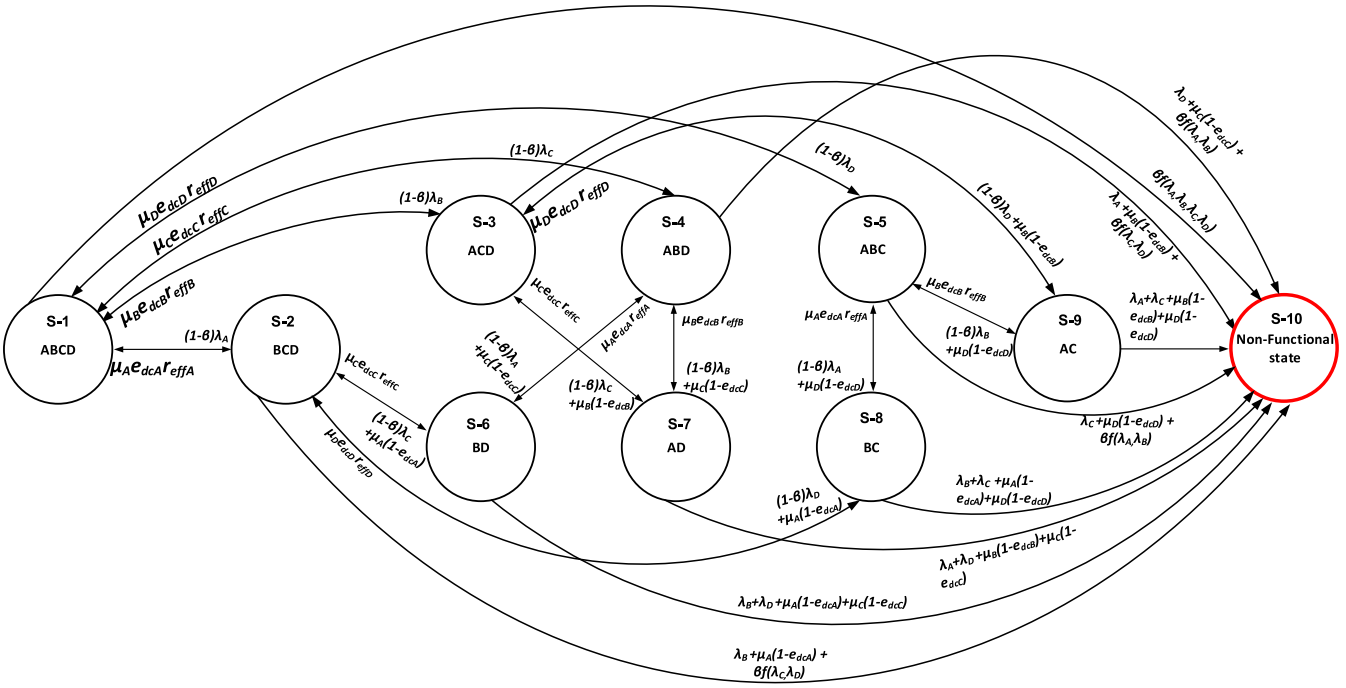

FIGURE 8. System transition diagram of the synchronous generator protection with imperfect repairs and CCFs based on Markov process.

Hence, given $X : R^n \rightarrow R^n$ as a linear map, its matrix form is given by (23) [49].

$$X(x) = \begin{pmatrix} X_1(x_1, \ldots, x_n) \\ \vdots \\ X_n(x_1, \ldots, x_n) \end{pmatrix} \tag{23}$$

Therefore, (23) can also be written in the form of (24),

$$X(x) = \begin{pmatrix} a_{11} & \cdots & a_{1n} \\ \vdots & \ddots & \vdots \\ a_{n1} & \cdots & a_{nn} \end{pmatrix} \begin{pmatrix} x_1 \\ \vdots \\ x_n \end{pmatrix} \tag{24}$$

So that (22) simplifies to (25).

$$x_{n+1} = X(x_n) = Ax_n \tag{25}$$

where A is the coefficient matrix comprising the elements (a_{ij}). Therefore, any change to the system variables based on some new variable requires the expression of x_i (for $i = 0, \ldots, n$) given by (8) [49], [50].

$$x_i = \sum_{j=1}^{n} m_{ij} y_j \quad \text{for } i = 0, \ldots, n), \tag{26}$$

which may also be expressed as given by (27),

$$x = My \tag{27}$$

where m_{ij} is an absolute constant $\forall$ i and j, implying a bijection such that M is a non-singular matrix. Thus, the columns m_i of M are linearly independent. Hence, x is given by (28).

$$x = \sum_{i=1}^{n} y_i m_i \tag{28}$$

It follows, therefore, that (23) simplifies to (29).

$$x_{n+1} = My_{n+1} = AMy_n \tag{29}$$

Consequently,

$$y_{n+1} = By_n \tag{30}$$

if A and B are similar matrices, such that

$$B = M^{-1}AM \tag{31}$$

where the matrix B is the Jordan form of matrix A [49], [50], [52]. The concepts and applications of matrix similarity and the Jordan form matrices to studying system dynamics are discussed in the following section.

VII. SYSTEM DYNAMICS AND CONVERGENCE OF MARKOV PROCESSES

Markov processes can be viewed as linear dynamical systems, where the i^{th} row of the transition probability matrix represents the system's state at time i [37], [38]. The impact of CCFs on the systems' dynamical behaviour and performance is analysed by prudently examining the behavioural dynamics of the system's transitions' probabilities. In considering (31), the transition probability matrix P can be written in the form of (32) [37], [38].

$$P = V \Lambda V^{-1} \tag{32}$$

where Λ is the diagonal eigenvalue $(\gamma_i \ldots \gamma_n)$ matrix of P associated with the linearly independent eigenvectors $(v_i \ldots v_n)$ in V. Thus, by association, at time step t, P^t is given by (33).

$$P^t = (V \Lambda^t V^{-1}) \tag{33}$$

where Λ^t is given by (34).

$$\Lambda^t = \begin{pmatrix} \gamma_1^t & 0 & \cdots & 0 \\ 0 & \gamma_2^t & \cdots & 0 \\ \vdots & \vdots & \ddots & \vdots \\ 0 & 0 & \cdots & \gamma_n^t \end{pmatrix} \tag{34}$$

It follows, therefore, that the system at time t given by $X(t)$ is represented by (35).

$$X(t) = c_1\gamma_1^t v_1 + c_2\gamma_2^t v_2 + \ldots + c_n\gamma_n^t v_n \tag{35}$$

Thus, it can be deduced from (35) that all terms with eigenvalues of magnitude less than one becomes zero at $t \to \infty$, while all terms whose eigenvalue magnitude equal one remain since a Markov transition probability matrix cannot have eigenvalues of greater than one [45], [51], [53]. Therefore, the number of eigenvalue magnitudes one represents the periodicity of the system, whereas the spectral gap between the eigenvalue magnitude one and the second largest eigenvalue(s) represent the system's rate of convergence [50], [53], [54].

The advantage of the proposed method is its ability to evaluate the quality of repairs, which can then be used to evaluate the effectiveness of maintenance and repair strategies. Similarly, the method can evaluate the adequacy of system diagnostic coverage during specification and design. This approach improves the results of recently published reliability studies of IEC 61850 based SCN architecture that employed combinatorial analysis techniques. Combinatorial analysis techniques cannot investigate the impact of CCF on systems with limited diagnostic coverage and low repair efficiency since they assume that repairs are fully effective. The following section presents the case studies results and discussions.

VIII. RESULTS AND DISCUSSIONS

Results and analysis of the impact of CCFs coupled with the quality of repairs on the reliability performance of the 'one-out-of-two' scheme configuration, depicted in Figure 7, are presented in this section. As presented in ISO 13849-1, three levels of diagnostic capabilities are investigated in determining the impact of repairs quality coupled with CCFs. The levels of system diagnostic coverages are presented in Table 3, where coverages of less than 60% are not denoted due to their ineffectiveness of the system's performance [55]–[58]. Thus, it is implied that system diagnostic capability should be at least 60% and above.

The following assumptions simplify the case studies and their analysis thereof:

a) Subsystems A and B are identical with equal diagnostic coverage levels.
b) One team maintains both subsystems A and B. Hence, they have equal repair efficiencies.
c) The system is fully functional at the beginning of the simulation (i.e., state S-1), cognizant that partial failures at the beginning of the simulation can be simulated if desired.

TABLE 3. Levels of diagnostic coverage and range.

Denotation	Range
None	$e_{dc} < 60\%$
Low	$60\% \leq e_{dc} < 90\%$
Medium	$90\% \leq e_{dc} < 99\%$
High	$99\% \leq e_{dc}$

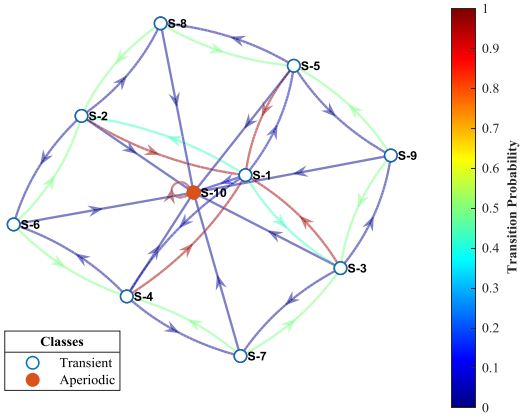

FIGURE 9. Scheme transitioning probabilities' diagram of the system at 99% diagnostic coverage.

The simulation results of the state transition probability diagrams are presented using the concept of state transition probabilities based on the ratio property, wherein for n number of events to occur in the next time step, the probability for the i^{th} event to occur first is given by (36) [59].

$$Pr(i^{th} \text{ is the first event}) = \frac{\lambda_i}{\lambda_1 + \lambda_2 + \ldots + \lambda_n} \tag{36}$$

A. HIGH DIAGNOSTIC COVERAGE

This case study assumes all subsystems have 99% diagnostic coverages. Figure 9 depicts the scheme's transitioning probabilities through its states when the repair efficiencies of the subsystems are 95%, whereas the common cause failure proportion level is 20%.

It is observable from Figure 9 that the system can transition into either state S-2 or S-3, and S-4 or S-5 with equal probabilities considering state S-1 as the initial system state. It is also observable that the system can transition into state S-10 from state S-1, even though the probability is very low. In addition, the system can transition into state S-10 from any of the partially functional states (viz S-2 to S-9). Similarly, to the impact of the CCF proportion rate, the probability is low. Thus, states S-1through to state S-9 are the transient states.

Moreover, the probability of the system transitioning back to states S-1 from states S-2, S-3, S-4 or S-5 is very high due to the high repair rate of the individual subsystems, of which the behaviour is similar for states S-6, S-7, S-8 and S-9 transitioning back to states S-2, S-3, S-4 or S-5, respectively. In order to enhance the readability of the system state

TABLE 4. State transition probabilities of the system at 99% diagnostic coverage.

	S-1	S-2	S-3	S-4	S-5	S-6	S-7	S-8	S-9	S-10	$\sum P_r$
S-1	0	0.4314	0.4314	0.0392	0.0392	0	0	0	0	0.0588	1
S-2	0.9690	0	0	0	0	0.0103	0	0.0103	0	0.0104	1
S-3	0.9690	0	0	0	0	0	0.0103	0	0.0103	0.0104	1
S-4	0.9690	0	0	0	0	0.0104	0.0104	0	0	0.0103	1
S-5	0.9690	0	0	0	0	0	0	0.0104	0.0104	0.0103	1
S-6	0	0.4947	0	0.4947	0	0	0	0	0	0.0106	1
S-7	0	0	0.4947	0.4947	0	0	0	0	0	0.0106	1
S-8	0	0.4947	0	0	0.4947	0	0	0	0	0.0106	1
S-9	0	0	0.4947	0	0.4947	0	0	0	0	0.0106	1
S-10	0	0	0	0	0	0	0	0	0	1	1

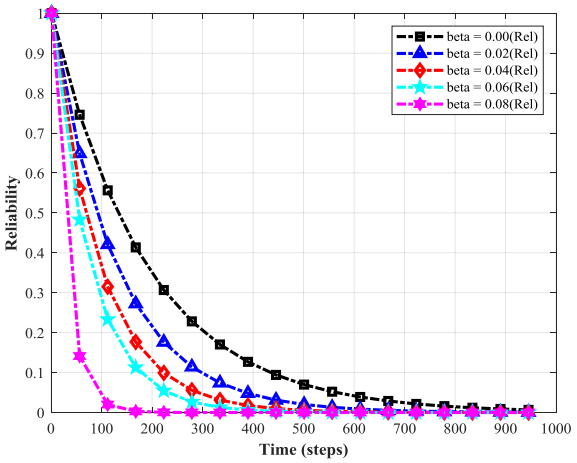

FIGURE 10. System reliability and unreliability based on the mean state transitions at 99% diagnostic capability.

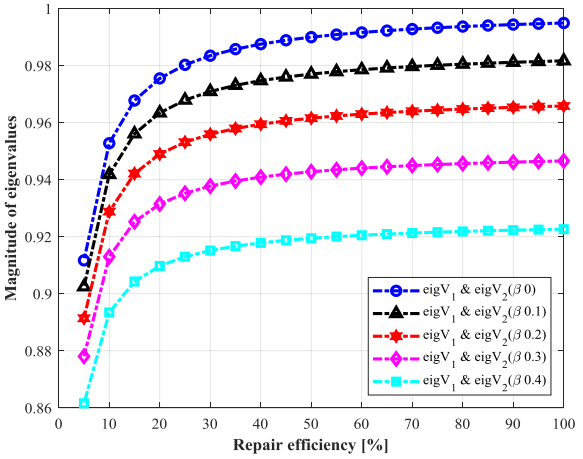

FIGURE 11. Eigenvalue magnitudes of the state transition probability matrix at 99% diagnostic capability.

transition probabilities, actual values are presented in Table 4. Figure 10 depicts the reliability curves of the system at various CCF levels represented by the β factor.

It can be observed that the MTTF considering state transitions of the system indicated by the 50% reliability level decreases with increasing CCF level, notwithstanding the impact reduction as the CCF level increases. Figure 11 depicts the magnitudes of eigenvalues 1 and 2 at various repair efficiency and β factor levels. The magnitudes of these eigenvalues are considered since they are the second-largest eigenvalues of the system that determines the system mean state transitions, given that an absorbing Markov chain always has an eigenvalue of magnitude one. The β factor levels do not impact eigenvalues of magnitude one and zero.

In addition, it can be observed that the repair efficiency is most effective at low levels, whereas the β factor reduces the eigenvalue magnitudes. The impact of the β factor is marginally uniform for all levels of repair efficiency, although pronounced at high repair efficiency levels. Thus, the β factor reduces the eigenvalue magnitudes for all eigenvalues greater than zero and less than 1, reducing the system's mean state transitions.

Figure 12 depicts the layout formation of the eigenvalues on the complex plane, illustrating a consistent formation of the eigenvalues for all β factor levels. Hence, the results indicate that the system is dynamically stable.

B. MEDIUM DIAGNOSTIC COVERAGE

This case study assumes the subsystems have 90% diagnostic coverage levels. Figure 13 depicts the scheme's transitioning probabilities through its states when the repair efficiencies of the subsystems are 95%, whereas the common cause failure proportion level is 20%, as in the previous case study.

As before, it is observable from Figure 13 that the system can transition into either state S-2 or S-3, and S-4 or S-5 with equal probabilities considering state S-1 as the initial system state. It is also observable that the system can transition into state S-10 from state S-1, even though the probability is very low. In addition, the system can transition into state S-10 from any of the partially functional states (viz S-2 to S-9). Similarly, to the impact of the CCF proportion rate, the probability is low. Thus, states S-1through to state S-9 are the transient states as in the previous case study. Moreover, the probability of the system transitioning back to states S-1 from states S-2,

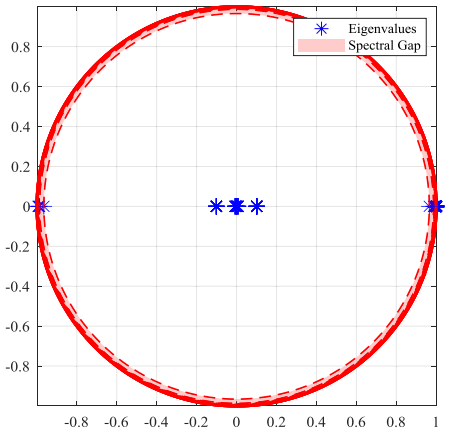

FIGURE 12. Eigenvalue layout formation and the spectral gap at 99% diagnostic coverage.

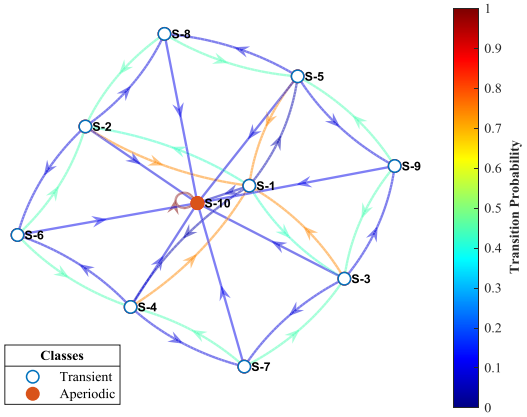

FIGURE 13. Scheme transitioning probabilities' diagram of the system at 90% diagnostic coverage.

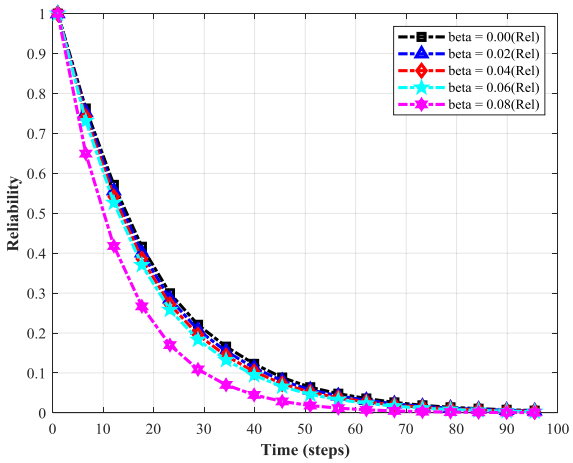

FIGURE 14. System reliability and unreliability based on the mean state transitions at 90% diagnostic coverage.

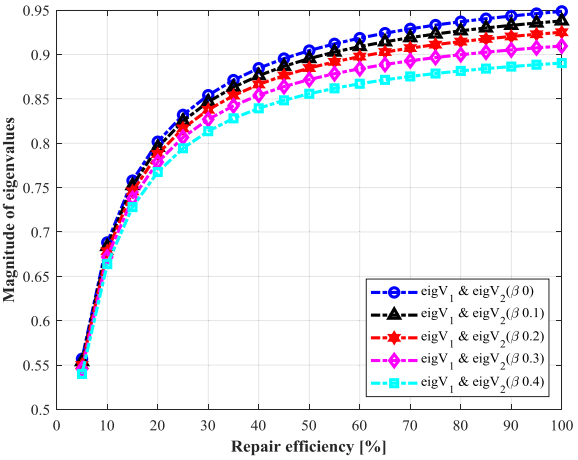

FIGURE 15. Eigenvalue magnitudes of the state transition probability matrix at 90% diagnostic coverage.

S-3, S-4 or S-5 is very high due to the high repair rate of the individual subsystems, of which the behaviour is similar for states S-6, S-7, S-8 and S-9 transitioning back to states S-2, S-3, S-4 or S-5, respectively.

Even so, the repair transitioning probabilities had reduced than when the diagnostic coverage was 99%, whereas the failure probabilities of the system have increased. As before, to enhance the readability of the system state transition probabilities of the system, actual values are presented in Table 5. Thus, states S-1 through S-9 are transient states. Moreover, the probability of the system transitioning back to states S-1 from states S-2, S-3, S-4 or S-5 remains relatively high due to the high repair rate of the individual subsystems, even though a reduction from the previous case study's results is noticeable.

A similar trend is noticeable when the system transitions back to states S-6, S-7, S-8 and S-9, transitioning back to states S-2, S-3, S-4 or S-5, respectively. Figure 14 depicts the reliability curves of the system at various CCF levels represented by the β factor. The system MTTF based on the mean state transitions decreases with increasing CCF level, notwithstanding the impact reduction as the CCF level increases. This behaviour is the same as in the previous case study. However, the mean state transitions have reduced significantly.

Moreover, the change in the mean state transition is much smaller than in the previous case study. Figure 15 depicts the eigenvalues 1 and 2 magnitudes at various repair efficiency and β factor levels. As before, the magnitudes of these eigenvalues are considered since they are the second-largest eigenvalues of the system that determines the system mean state transitions, given that an absorbing Markov chain always has an eigenvalue of magnitude one. The β factor levels do not impact eigenvalues of magnitude one and zero.

Again, it can be observed in Figure 16 that the repair efficiency is most effective at low levels, whereas the β factor reduces the eigenvalue magnitudes. The impact of the β factor is not uniform across repair efficiency levels. Instead, the β factor has a minimal impact at low repair efficiency levels, which increases as the repair efficiency level increase. Thus, the β factor reduces the eigenvalue magnitudes for all eigenvalues greater than zero and less than 1, which reduces the system's mean state transitions. Figure 15 depicts the complex plane formation of the eigenvalues, illustrating a

TABLE 5. State transition probabilities of the system at 90% diagnostic coverage.

	S-1	S-2	S-3	S-4	S-5	S-6	S-7	S-8	S-9	S-10	$\sum P_r$
S-1	0	0.4314	0.4314	0.0392	0.0392	0	0	0	0	0.0588	1
S-2	0.7402	0	0	0	0	0.0866	0	0.0866	0	0.0866	1
S-3	0.7402	0	0	0	0	0	0.0866	0	0.0866	0.0866	1
S-4	0.7402	0	0	0	0	0.0866	0.0866	0	0	0.0866	1
S-5	0.7402	0	0	0	0	0	0	0.0866	0.0866	0.0866	1
S-6	0	0.4476	0	0.4476	0	0	0	0	0	0.1047	1
S-7	0	0	0.4476	0.4476	0	0	0	0	0	0.1047	1
S-8	0	0.4476	0	0	0.4476	0	0	0	0	0.1047	1
S-9	0	0	0.4476	0	0.4476	0	0	0	0	0.1047	1
S-10	0	0	0	0	0	0	0	0	0	1	1

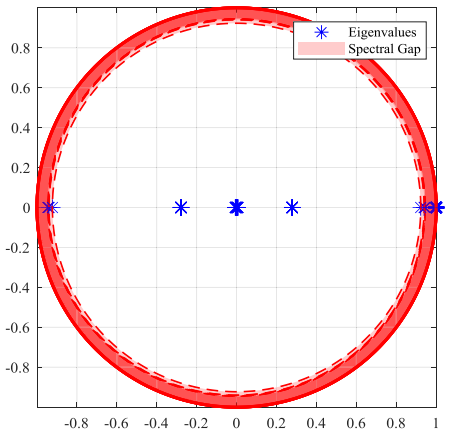

FIGURE 16. Eigenvalue layout formation and the spectral gap at 90% diagnostic coverage.

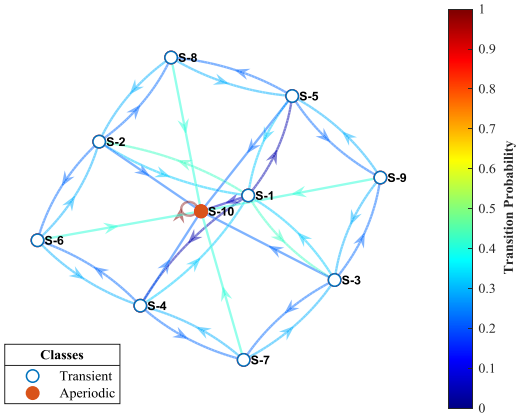

FIGURE 17. Scheme transitioning probabilities' diagram of the system at 60% diagnostic coverage.

consistent formation of the eigenvalues for all β factor levels, as in the previous case study. Hence, the results indicate that the system is dynamically stable even though its diagnostic coverage has been reduced, causing the spectral gap to increase.

C. LOW DIAGNOSTIC COVERAGE

This case study assumes the subsystems have 60% diagnostic coverage. Figure 17 depicts the scheme's transitioning

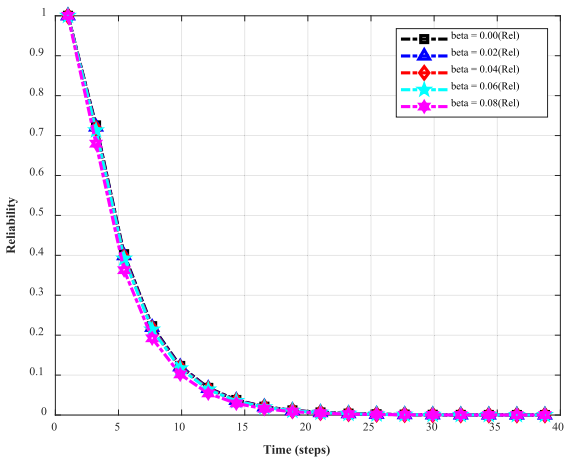

FIGURE 18. System reliability and unreliability based on the mean state transitions at 60% diagnostic capability.

probabilities through its states when the repair efficiencies of the subsystems are 95%, whereas the common cause failure proportion level is 20%. As before, it is observable from Figure 17 that the system can transition to either state S-2 o3 S-3, and S-4 or S-5 with equal probabilities considering state S-1 as the initial system state. The system can also easily transition into state S-10 from any state S-1 through to S-9 because the probability has relatively increased than in the previous case studies resulting from the increased unknown system errors. States S-1 through to S-9 remain transient even though the diagnostic coverage has significantly reduced following the diagnostic coverage reduction. Figure 18 depicts the reliability curves of the system at various CCF levels represented by the β factor. Similarly, to the impact of the CCF proportion rate, the probability is low. Thus, states S-1 through to S-9 are the transient states as in the previous case studies. In contrast, the probability of the system transitioning back to states S-1 from states S-2, S-3, S-4 or S-5 has reduced significantly even though the high repair rate is very high as a result of poor system diagnostic coverage, of which the behaviour is similar for states S-6, S-7, S-8 and S-9 transitioning back to states S-2, S-3, S-4 or S-5, respectively.

Consequently, the mean state transitions have significantly reduced than in the previous case studies. States S-1 through

TABLE 6. State transition probabilities of the system at 60% diagnostic coverage.

	S-1	S-2	S-3	S-4	S-5	S-6	S-7	S-8	S-9	S-10	$\sum P_r$
S-1	0	0.4314	0.4314	0.0392	0.0392	0	0	0	0	0.0588	1
S-2	0.3220	0	0	0	0	0.2260	0	0.2260	0	0.2260	1
S-3	0.3220	0	0	0	0	0	0.2260	0	0.2260	0.2260	1
S-4	0.3220	0	0	0	0	0.2260	0.2260	0	0	0.2260	1
S-5	0.3220	0	0	0	0	0	0	0.2260	0.2260	0.2260	1
S-6	0	0.2938	0	0.2938	0	0	0	0	0	0.4124	1
S-7	0	0	0.2938	0.2938	0	0	0	0	0	0.4124	1
S-8	0	0.2938	0	0	0.2938	0	0	0	0	0.4124	1
S-9	0	0	0.2938	0	0.2938	0	0	0	0	0.4124	1
S-10	0	0	0	0	0	0	0	0	0	1	1

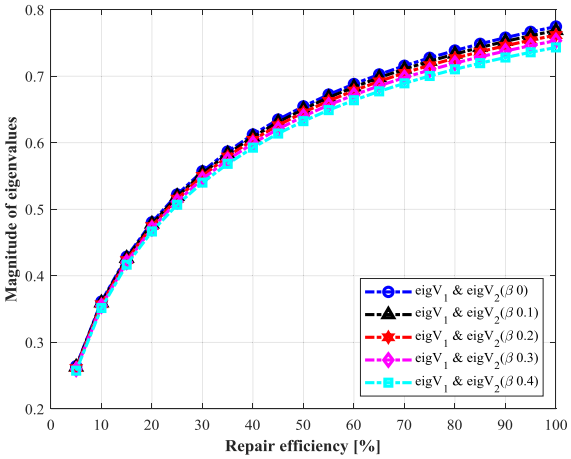

FIGURE 19. Magnitudes of eigenvalues of the state transition probability matrix at 60% diagnostic capability.

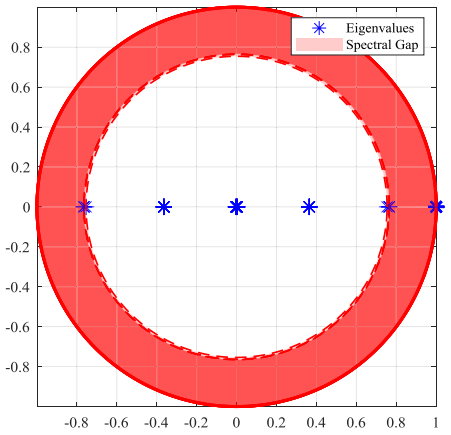

FIGURE 20. Eigenvalue layout formation and the spectral gap at 60% diagnostic capability.

to S-9 remain transient even though the diagnostic coverage has significantly reduced. In addition, the probabilities of the system transitioning back to states S-1 from states S-2, S-3, S-4 or S-5 have reduced significantly following the diagnostic coverage reduction. Figure 18 depicts the reliability curves of the system at various CCF levels represented by the β factor.

As in the previous case studies, the system's MTTF based on the mean state transitions decreases with increasing CCF levels. This behaviour is the same as in the previous case studies. The mean state transitions have significantly reduced even further.

As before, to enhance the readability of the system state transition probabilities of the system, actual values are presented in Table 6. In contrast, the probability of the system transitioning back to states S-1 from states S-2, S-3, S-4 or S-5 has reduced. The magnitudes of eigenvalues 1 and 2 at various repair efficiencies and levels of β factor are depicted in Figure 19. As before, the magnitudes of these eigenvalues are considered since they are the second-largest eigenvalues of the system that determines the system mean state transitions, given that an absorbing Markov chain always has an eigenvalue of magnitude one. The β factor levels do not impact eigenvalues of magnitude one and zero.

It is noticeable in Figure 19 that the repair efficiency is most effective at low levels, whereas the β factor reduces the eigenvalue magnitudes. The impact of the β factor is not uniform across repair efficiency levels, as in the previous case studies. In addition, the β factor has a minimal impact at low repair efficiency levels, which marginally increases as the repair efficiency level increase. Thus, the β factor reduces the eigenvalue magnitudes for all eigenvalues greater than zero and less than 1, which reduces the system's mean state transitions. Even so, the impact is less than in the previous case studies. Figure 19 depicts the complex plane formation of the eigenvalues, illustrating a consistent formation of the eigenvalues for all β factor levels. Hence, the results indicate that the system is dynamically stable even though its diagnostic coverage has been reduced further to 60%, causing the spectral gap to increase while reducing the mean state transitions.

IX. CONCLUSION

The impact of CCFs coupled with the quality of repairs on the reliability performance of IEC 61850 based SCN architecture is successfully investigated using the Markov process and Linear Dynamical System. The impact of engineering design

considerations and coupling factors was modelled using the beta factor model to enable various CCF levels to be investigated. The diagnostic coverage level of the system is based on the ISO 13849-1, the standard for machinery safety. The results of the case studies indicate that engineering design considerations and coupling factors negatively impact the system's reliability performance, notably for mission-critical applications with high diagnostic coverage. The results also indicate that engineering design considerations and coupling factors have less impact when the system diagnostic coverage is low, specifically at low repair efficiency levels. However, the impact becomes more pronounced as the repair efficiency increases, as observed from the responses of the eigenvalue magnitudes when the β factor is increased. Thus, it is critical to ensure minimum impact of common engineering design considerations and coupling factors by diversifying the system's subsystems, as well as ensuring a high independence level among the subsystems.

The proposed model in this research proved to be very effective in investigating the effectiveness of the quality of repairs and CCF, and hence it would apply to more complex systems such as the IEC 61850 based SCN for inter-substation applications, which is more complex than the intra-bay SCN application and is planned to be done as future research work. Future research is also planned to investigate the sensitivity of the system performance to the quality of repairs and CCF.

REFERENCES

[1] X. Yang, N. Das, and S. Islam, "Analysis of IEC 61850 for a reliable communication system between substations," in *Proc. Australas. Universities Power Eng. Conf. (AUPEC)*, Sep. 2013, pp. 1–6, doi: 10.1109/aupec.2013.6725482.

[2] V. C. Mathebula and A. K. Saha, "Mission critical safety functions in IEC-61850 based substation automation system—A reliability review," *Int. J. Eng. Res. Afr.*, vol. 48, pp. 149–161, May 2020, doi: 10.4028/www.scientific.net/jera.48.149.

[3] K. Brand, M. Ostertag, and W. Wimmer, "Safety related, distributed functions in substations and the standard IEC 61850," in *Proc. IEEE Bologna Power Tech Conf.*, vol. 2, Jun. 2003, pp. 260–264, doi: 10.1109/PTC.2003.1304319.

[4] J. V. Bukowski and R. Chalupa, "Calculating an appropriate multiplier for $\beta\lambda$ when modeling common cause failure in triplex systems," in *Proc. Annu. Rel. Maintainability Symp. (RAMS)*, San Jose, CA, USA, Jan. 2010, pp. 1–5, doi: 10.1109/RAMS.2010.5447996.

[5] J. R. Belland, "Modeling common cause failures in diverse components with fault tree applications," in *Proc. Annu. Rel. Maintainability Symp. (RAMS)*, Orlando, FL, USA, Jan. 2017, pp. 1–6, doi: 10.1109/RAM.2017.7889659.

[6] L. Xing and W. Wang, "Probabilistic common-cause failures analysis," in *Proc. Annu. Rel. Maintainability Symp.*, Las Vegas, NV, USA, Jan. 2008, pp. 354–358, doi: 10.1109/RAMS.2008.4925821.

[7] D. Kumar, G. L. Pahuja, and J. K. Quamara, "Chemical reactor safety system reliability under common cause failure," in *Proc. 3rd IEEE Int. Conf. Recent Trends Electron., Inf. Commun. Technol. (RTEICT)*, Bengaluru, India, May 2018, pp. 2534–2537, doi: 10.1109/RTEICT42901.2018.9012319.

[8] M. Kumar, A. Kabra, G. Karmakar, and P. P. Marathe, "A review of defences against common cause failures in reactor protection systems," in *Proc. 4th Int. Conf. Rel., INFOCOM Technol. Optim. (ICRITO) (Trends Future Directions)*, Noida, India, Sep. 2015, pp. 1–6, doi: 10.1109/ICRITO.2015.7359232.

[9] M. Pourali, "Incorporating common cause failures in mission-critical facilities reliability analysis," *IEEE Trans. Ind. Appl.*, vol. 50, no. 4, pp. 2883–2890, Jul. 2014, doi: 10.1109/TIA.2013.2295472.

[10] P. Hokstad and M. Rausand, *Common Cause Failure Modeling: Status and Trends*. London, U.K.: Springer, 2008.

[11] A. Zhang, H. Srivastav, A. Barros, and Y. Liu, "Study of testing and maintenance strategies for redundant final elements in SIS with imperfect detection of degraded state," *Rel. Eng. Syst. Saf.*, vol. 209, May 2021, Art. no. 107393, doi: 10.1016/j.ress.2020.107393.

[12] Q. M. N. Amjad, M. Zubair, and G. Heo, "Modeling of common cause failures (CCFs) by using beta factor parametric model," in *Proc. Int. Conf. Energy Syst. Policies (ICESP)*, Islamabad, Pakistan, Nov. 2014, doi: 10.1109/ICESP.2014.7347004.

[13] J. Qin, R. Gu, and G. Li, "Reliability modeling of incomplete common cause failure systems subject to two common causes," in *Proc. IEEE Int. Conf. Ind. Eng. Manage. (IEEM)*, Singapore, Dec. 2017, pp. 1906–1910, doi: 10.1109/IEEM.2017.8290223.

[14] Q. Shao, S. Yang, C. Bian, and X. Gou, "Formal analysis of repairable phased-mission systems with common cause failures," *IEEE Trans. Rel.*, vol. 70, no. 1, pp. 1–12, Nov. 2020, doi: 10.1109/tr.2020.3032178.

[15] A. Khavnekar, S. Wagh, and A. More, "Comparative analysis of IEC 61850 edition-I and II standards for substation automation," in *Proc. IEEE Int. Conf. Comput. Intell. Comput. Res. (ICCIC)*, Dec. 2015, pp. 1–6, doi: 10.1109/ICCIC.2015.7435756.

[16] A. T. A. Pereira, L. A. C. Lisboa, and A. M. N. Lima, "Strategies and techniques applied to IEC 61850 based DSAS architectures," in *Proc. 13th Int. Conf. Develop. Power Syst. Protection (DPSP)*, Mar. 2016, pp. 1–5, doi: 10.1049/cp.2016.0009.

[17] S. M. S. Hussain, M. A. Aftab, and I. Ali, "A novel PRP based deterministic, redundant and resilient IEC 61850 substation communication architecture," *Perspect. Sci.*, vol. 8, pp. 747–750, Sep. 2016, doi: 10.1016/j.pisc.2016.06.077.

[18] J. A. Araujo, J. Lazaro, A. Astarloa, A. Zuloaga, and J. I. Garate, "PRP and HSR for high availability networks in power utility automation: A method for redundant frames discarding," *IEEE Trans. Smart Grid*, vol. 6, no. 5, pp. 2325–2332, Sep. 2015.

[19] H. Ngo, H.-S. Yang, D.-W. Ham, J. Rhee, Y. An, J. Han, Y. Lee, and N. Lee, "An improved high-availability seamless redundancy (HSR) for dependable substation automation system," in *Proc. 16th Int. Conf. Adv. Commun. Technol.*, Feb. 2014, pp. 921–927, doi: 10.1109/ICACT.2014.6779094.

[20] S. Mnukwa and A. K. Saha, "SCADA and substation automation systems for the port of Durban power supply upgrade," in *Proc. Int. SAUPEC/RobMech/PRASA Conf.*, Cape Town, South Africa, Jan. 2020, doi: 10.1109/SAUPEC/RobMech/PRASA48453.2020.9041078.

[21] R. M. Rahat, M. H. Imam, and N. Das, "Comprehensive analysis of reliability and availability of sub-station automation system with IEC 61850," in *Proc. Int. Conf. Robot., Elect. Signal Process. Techn.*, Jan. 2019, pp. 406–411, doi: 10.1109/ICREST.2019.8644416.

[22] Y. Zhang, A. Sprintson, and C. Singh, "An integrative approach to reliability analysis of an IEC 61850 digital substation," in *Proc. IEEE Power Energy Soc. Gen. Meeting*, Jul. 2012, pp. 1–8, doi: 10.1109/PESGM.2012.6345699.

[23] V. C. Mathebula and A. K. Saha, "Reliability and availability of multichannel IEC-61850 substation communication networks for mission-critical applications," *Int. J. Eng. Res. Afr.*, vol. 51, pp. 199–216, Nov. 2020, doi: 10.4028/www.scientific.net/JERA.51.199.

[24] N. Das and S. Islam, "Analysis of power system communication architectures between substations using IEC 61850," in *Proc. 5th Brunei Int. Conf. Eng. Technol. (BICET)*, Nov. 2014, pp. 1–8, doi: 10.1049/cp.2014.1060.

[25] N. Das, W. Ma, and S. Islam, "Analysis of end-to-end delay characteristics for various packets in IEC 61850 substation communications system," in *Proc. Australas. Universities Power Eng. Conf. (AUPEC)*, Wollongong, NSW, Australia, Sep. 2015, pp. 1–5, doi: 10.1109/AUPEC.2015.7324831.

[26] T. J. Wong and N. Das, "Modelling and analysis of IEC 61850 for end-to-end delay characteristics with various packet sizes in modern power substation systems," in *Proc. 5th Brunei Int. Conf. Eng. Technol. (BICET)*, Nov. 2014, pp. 1–6, doi: 10.1049/cp.2014.1073.

[27] S. Kumar, N. Das, and S. Islam, "Performance analysis of substation automation systems architecture based on IEC 61850," in *Proc. Australas. Universities Power Eng. Conf. (AUPEC)*, Sep. 2014, pp. 1–6, doi: 10.1109/AUPEC.2014.6966532.

[28] A. Albarakati, C. Robillard, M. Karanfil, M. Kassouf, M. Debbabi, A. Youssef, M. Ghafouri, and R. Hadjidj, "Security monitoring of IEC 61850 substations using IEC 62351-7 network and system management," in *Proc. IEEE Int. Conf. Commun., Control, Comput. Technol. Smart Grids (SmartGridComm)*, early access, May 19, 2019, doi: 10.1109/SmartGridComm.2019.8909710.

[29] J. Stark, W. Wimmer, and K. Majer, "Switchgear optimization using IEC 61850-9-2," in *Proc. 22nd Int. Conf. Exhib. Electr. Distrib.*, Jun. 2013, pp. 1–4.
[30] S. Kumar, N. Das, and S. Islam, "High performance communication redundancy in a digital substation based on IEC 62439-3 with a station bus configuration," in *Proc. Australas. Universities Power Eng. Conf. (AUPEC)*, Sep. 2015, pp. 1–5, doi: 10.1109/AUPEC.2015.7324838.
[31] B. Yunus, A. Musa, H. S. Ong, A. R. Khalid, and H. Hashim, "Reliability and availability study on substation automation system based on IEC 61850," in *Proc. IEEE 2nd Int. Power Energy Conf.*, Dec. 2008, pp. 148–152, doi: 10.1109/PECON.2008.4762462.
[32] M. G. Kanabar and T. S. Sidhu, "Reliability and availability analysis of IEC 61850 based substation communication architectures," in *Proc. IEEE Power Energy Soc. Gen. Meeting*, Jul. 2009, pp. 1–8, doi: 10.1109/PES.2009.5276001.
[33] M. Mekkanen, R. Virrankoski, M. Elmusrati, and E. Antila, "Reliability evaluation and comparison for next-generation substation function based on IEC 61850 using Monte Carlo simulation," in *Proc. 1st Int. Conf. Commun., Signal Process., Appl. (ICCSPA)*, Feb. 2013, pp. 1–6, doi: 10.1109/ICCSPA.2013.6487306.
[34] L. Andersson, K.-P. Brand, C. Brunner, and W. Wimmer, "Reliability investigations for SA communication architectures based on IEC 61850," in *Proc. IEEE Russia Power Tech*, Jun. 2005, pp. 1–7, doi: 10.1109/PTC.2005.4524707.
[35] M. C. Magro, P. Pinceti, and L. Rocca, "Can we use IEC 61850 for safety related functions?" in *Proc. IEEE 16th Int. Conf. Environ. Electr. Eng. (EEEIC)*, Jun. 2016, pp. 1–6, doi: 10.1109/EEEIC.2016.7555402.
[36] M. C. Magro, P. Pinceti, L. Rocca, and G. Rossi, "Safety related functions with IEC 61850 GOOSE messaging," *Int. J. Electr. Power Energy Syst.*, vol. 104, pp. 515–523, Jan. 2019, doi: 10.1016/j.ijepes.2018.07.033.
[37] V. C. Mathebula and A. K. Saha, "Multi-state IEC-61850 substation communication network based on Markov partitions and symbolic dynamics," *Sustain. Energy, Grids Netw.*, vol. 26, Jun. 2021, Art. no. 100466, doi: 10.1016/j.segan.2021.100466.
[38] V. C. Mathebula and A. K. Saha, "Impact of imperfect repairs and diagnostic coverage on the reliability of multi-channel IEC-61850 substation communication network," *IEEE Access*, vol. 9, pp. 2758–2769, 2021, doi: 10.1109/ACCESS.2020.3047781.
[39] V. C. Mathebula and A. K. Saha, "Responsiveness of multi-channel IEC-61850 substation communication network reliability performance to changes in repair factors," *IEEE Access*, vol. 9, pp. 789–800, 2021, doi: 10.1109/ACCESS.2020.3046950.
[40] V. C. Mathebula and A. K. Saha, "Sensitivity and elasticity of multi-channel IEC-61850 substation communication networks to imperfect repairs," *Sustain. Energy, Grids Netw.*, vol. 26, Jun. 2021, Art. no. 100443, doi: 10.1016/j.segan.2021.100443.
[41] V. C. Mathebula. (2019). *Application of Bus Transfer Schemes to Stabilise Power Supply in a Coal Fired Power Plant Unit Auxiliary Reticulation*. Durban, South Africa. [Online]. Available: https://researchspace.ukzn.ac.za/handle/10413/17029
[42] V. C. Mathebula and A. K. Saha, "Coal fired power plant in-phase bus transfer simulation of forced and induced draught fan motors," in *Proc. Southern Afr. Universities Power Eng. Conf./Robot. Mechatronics/Pattern Recognit. Assoc. South Afr. (SAUPEC/RobMech/PRASA)*, Jan. 2019, pp. 293–298, doi: 10.1109/RoboMech.2019.8704820.
[43] V. C. Mathebula and A. K. Saha, "Development of in-phase bus transfer scheme using MATLAB simulink," in *Proc. Southern Afr. Universities Power Eng. Conf./Robot. Mechatronics/Pattern Recognit. Assoc. South Afr. (SAUPEC/RobMech/PRASA)*, Bloemfontein, South Africa, Jan. 2019, pp. 275–280, doi: 10.1109/RoboMech.2019.8704815.
[44] S. A. Kunsman, N. Powers, and B. Vasudevan, "Protection and control system use of non-conventional instrument transformers and process bus," *Int. Electr. Test. Assoc. J. NETA World*, pp. 77–84, 2017. [Online]. Available: https://library.e.abb.com/public/5686c3fc42b94c04910b024d91054a85/Netaworld%20digital%20substation%202017.pdf
[45] K. T. Alligood, T. D. Sauer, and J. A. Yorke, *An Introduction to Dynamical Systems and Chaos*. New York, NY, USA: Springer-Verlag, 1996.
[46] R. A. Horn and C. R. Johnson, *Matrix Analysis*, 2nd ed. Cambridge, U.K.: Cambridge Univ. Press, 2013.
[47] R. Billinton and R. N. Allan, *Reliability Evaluation of Engineering Systems: Concepts and Techniques*, vol. 5, no. 1, 2nd ed. New York, NY, USA: Plenum, 1983.
[48] R. Smith and M. Modarres, "A physics of failure approach to common cause failure considering component degradation," in *Proc. Annu. Rel. Maintainability Symp. (RAMS)*, Palm Springs, CA, USA, Jan. 2020, pp. 1–6, doi: 10.1109/RAMS48030.2020.9153651.
[49] W. Hu, "Dynamical systems," *Vertical Integration of Research and Education*. Chicago, IL, USA: Univ. Chicago, 2009, pp. 1–15. [Online]. Available: https://math.uchicago.edu/ may/VIGRE/VIGRE2009/REUPapers/Hu.pdf
[50] E. R. Scheinerman, *Invitation To Dynamical Systems*. New York, NY, USA: Dover, 2013.
[51] D. Margalit and J. Rabinoff. (2019). *Interactive Linear Algebra*. Georgia Institute of Technology. Atlanta, Georgia. [Online]. Available: https://textbooks.math.gatech.edu/ila/subspaces.html.
[52] M. R. Spiegel, *Advanced Mathematics for Engineers and Scientists*. Singapore: Schaum's Outline Series, 1983.
[53] R. G. Gallager, *Stochastic Processes Theory for Applications*. Cambridge, U.K.: Cambridge Univ. Press, 2013.
[54] R. L. Tweedie, "Criteria for classifying general Markov chains," *Adv. Appl. Probab.*, vol. 8, no. 4, pp. 737–771, 1976.
[55] A. Porras-Vázquez and J. A. Romero-Pérez, "A new methodology for facilitating the design of safety-related parts of control systems in machines according to ISO 13849: 2006 standard," *Reliab. Eng. Syst. Saf.*, vol. 174, pp. 60–70, Jun. 2018, doi: 10.1016/j.ress.2018.02.018.
[56] T. Fukuda, M. Hirayama, N. Kasai, and K. Sekine, "Evaluation of operative reliability of safety-related part of control system of machine and safety level," in *Proc. SICE Annu. Conf.*, Sep. 2007, pp. 2480–2483, doi: 10.1109/SICE.2007.4421406.
[57] P. Lereverend, "Inside the standardization jungle: IEC 62061 and ISO 13849-1, complementary or competing?" in *Proc. 5th Petroleum Chem. Ind. Conf. Eur. Electr. Instrum. Appl.*, Weimar, Germany, Jun. 2008, pp. 1–5, doi: 10.1109/PCICEUROPE.2008.4563534.
[58] H. Srivastav, A. Barros, and M. A. Lundteigen, "Modelling framework for performance analysis of SIS subject to degradation due to proof tests," *Rel. Eng. Syst. Saf.*, vol. 195, Mar. 2020, Art. no. 106702, doi: 10.1016/j.ress.2019.106702.
[59] J. F. Kitchin, "Practical Markov modeling for reliability analysis," in *Proc. Annu. Rel. Maintainability Symp.*, Jan. 1988, pp. 290–296, doi: 10.1109/arms.1988.196463.

VONANI CLIVE MATHEBULA received the B.Com. degree in finance from the University of South Africa and the B.Sc. and M.Sc. degrees in electrical engineering from the University of KwaZulu-Natal, Durban, South Africa, where he is currently pursuing the Ph.D. degree in electrical engineering. He is a practising engineer with over 19 years of experience in steel making and power generation industries. He is a registered Professional Engineer with the Engineering Council of South Africa. His research interests include advances in power systems and the reliability of substation communication systems for mission-critical applications in power distribution centres.

AKSHAY KUMAR SAHA (Member, IEEE) is currently an Associate Professor and an Academic Leader of research and higher degrees at the School of Engineering, University of KwaZulu-Natal, Durban, South Africa. He is also a registered Professional Engineer with the Engineering Council of South Africa and a fellow of South African Institute of Electrical Engineers, South African Academy of Engineering. He is a Senior Member of SAIMC and an Individual Member Cigre. His research works are related to advances of power systems in various areas including engineering education. He has published more than 30 articles in top-tier international journals and over 100 international conference papers in relevant areas. He was awarded the Best Lecturer Electrical Engineering by the School of Engineering, in 2013–2014 and 2016–2019, and the Research Excellence Award by the University of KwaZulu-Natal in the years 2015–2019. He is acting as an editorial board member for a number of top-tier international journals.